Research Article

SOHAG JOURNAL OF SCIENCES

https://doi.org/10.21608/sjsci.2023.211358.1080

Development of Novel Guanidine Iron (III) Complexes as a Powerful Catalyst for the Synthesis of Tetrazolo[1,5-*a*]pyrimidine by Green Protocol

Mahmoud Abd El Aleem Ali Ali El-Remaily[1,*], O. Elhady[1], Thomas Nady A. Eskander[1], Shaaban K Mohamed[3,4], Ahmed M. Abu- Dief[1,2]

[1] *Department of Chemistry, Faculty of Science, Sohag University, Sohag 82524 Egypt*
[2] *Chemistry Department, College of Science, Taibah University, P.O. Box 344, Madinah, Saudi Arabia*
[3] *Chemistry and Environmental Division, Manchester Metropolitan University, Manchester, United Kingdom*
[4] *Chemistry Department, Faculty of Science, Minia University, El-Minia, Egypt*
**E-mail: mahmoud_ali@science.sohag.edu.eg*

Received: 21st May 2023, **Revised:** 26th July 2023, **Accepted:** 18th August 2023
Published online: 1st September 2023

Abstract: The design of the structure of a coordination compound (catalyst) is of crucial importance for its catalytic applications. This paper presents a series of newly synthesized iron (III) complexes, including (benzothiazol-guanidine-Fe), (benzothiazol-imidazol-Fe), and (benzothiazol-pyrimidin-Fe), as potential catalysts for various organic reactions. To confirm their structures, the complexes were characterized using a variety of spectroscopic methods, such as FT-IR, ^{1}H-NMR, ^{13}C-NMR, CHN elemental analysis, electronic spectra, TGA, molar conductivity, and magnetic moment. Spectroscopy and other analytical studies reveal distorted octahedral geometry in iron complexes. In order to ascertain the kinetic and thermodynamic properties of complexes, the Coats-Redfern method was used. Further research was done into these complexes' catalytic abilities for the environmentally friendly synthesis of 7-amino-4,5-dihydro-tetrazolo[1,5-*a*]pyrimidine-6-carbonitrile derivatives using aromatic aldehyde, malononitrile, and 5-aminotetrazole as reactants. The reactions were conducted in a compassionate environment using a green solvent. The outcomes demonstrated the excellent catalytic activity and selectivity of the complexes, which led to good yields of the intended products. As a result, the study offers useful information on the novel iron (III) complexes' synthetic uses, and the creation of effective and environmentally acceptable catalysts, and emphasizes their potential as powerful catalysts for a variety of organic transformations. This strategy's simplicity, safety, commercially accessible catalyst, stability, fast reaction time, and outstanding yields may be used in the industry in the future.
Keywords: Guanidine iron (III) complexes, environmentally, tetrazolo[1,5-*a*]pyrimidine.

1. Introduction

Multicomponent reactions (MCR) [1-3] refer to processes in which several reactants interact to produce a single molecule in which the majority of the original materials' atoms are preserved. Essentially, the most beneficial multicomponent reactions are those that generate a single complex molecule (or cyclic configuration by simply adding one reactant to another without separating the intermediate [4]. Multicomponent Reactions (MCR) can be conducted in several techniques, such as transition metal catalyzed MCR, non-metal catalyzed MCR acid catalyzed MCR and nanoparticles catalyzed MCR [5,6]. Many types of heterocyclic structures were developed employing metal-catalyzed multicomponent impacts, which provided straightforward workup processes and high yields of isolated products [7-9].

Transition metal complexes have been extensively used as catalysts in multicomponent reactions (MCRs) due to their high catalytic activity and versatility. MCRs are reactions that involve the simultaneous reaction of three or more reactants to form a single product in one step. The use of transition metal complexes can catalyze MCRs through a variety of mechanisms, such as Lewis's acid activation, oxidative addition, and stereoselectivity of the reactants **[10].** These mechanisms can lead to increased reaction rates, selectivity, and yield. One of the key advantages of using transition metal complexes as catalysts in MCRs is their ability to act as both Lewis acids and bases. This allows them to activate and coordinate multiple reactants simultaneously, leading to the formation of various organic molecules with high efficiency and selectivity [11]. Iron-based catalysts, which are toxicologically low, and highly complex stable, meet the criteria for green chemistry when used in catalytic processes [9].

Iron catalysts containing ligands that function as nitrogen donors to stabilize them are a good candidate. Thesis complexes with cleverly crafted N donor ligands have been employed as catalysts in a broad spectrum of investigations. Moreover, considering iron's large natural availability and essential function in vital biological processes, which renders it non-toxic, inexpensive, and eco-friendly. They are more attractive as catalyst frameworks than other transition metals. In this work, we go into great depth on how to use iron-based catalysts to create green, benign, secure, and environmentally

beneficial reactions. Due to our continuing studies on the production of MCRs [13–15], the new Fe(II) complex's catalytic capability will be indicated here by the combination of an aromatic aldehyde, malononitrile, and 5-amino tetrazole in the straightforward and very effective one-pot synthesis for obtaining 7-amino-4,5-dihydro-tetrazolo[1,5-*a*]pyrimidine-6-carbonitrile derivatives. The beneficial properties of the recommended catalyst are primarily consisted of using a green solvent (H_2O/ethanol), a quicker reaction time, and excellent product yields. It also demonstrated that in the synthesis of 7-amino-4,5-dihydro-tetrazolo[1,5-*a*]pyrimidine-6-carbonitrile derivatives, iron-based catalysts outperformed other Lewis acids and basic catalysts. They are preferred because of their progressive changes and connections with a variety of operational groupings.

By the methodologies described above and as part of our ongoing research, we aimed to add success to the catalytic history of Fe (III) complexes by synthesizing bioactive heterocyclic molecules through multicomponent reactions. Because of its merits of being environmentally benign, readily accessible, and cost-effective, the Fe (III) complex seems to be a promising reusable catalyst in the facile one-pot synthesis of 7-amino-4,5-dihydro-tetrazolo[1,5-*a*]pyrimidine-6-carbonitrile derivatives through a three-component coupling reaction (involving an aromatic aldehyde, aminotetrazolo, and malononitrile) by green protocol.

2. Materials and methods

2.1. Reagents, Instrumentation, and Methods

All substances and ingredients were utilized exactly as Alfa Aesar or Sigma Aldrich had supplied them. The supporting material included descriptions of each instrument as well as details of the observations. In the discussion section, there will be a separate list of other critical needs.

2.2. Synthesis of ligands L_2 and L_3

Benzothiazol-guanidine (15 mmol, 2.88 g) was mixed with ethyl bromo acetate (15 mmol, 2.50 g), acetylacetone (15 mmol, 1.5 mL), and small droplets of glacial CH_3COOH as a benign catalyst. Following that, each reactant was added, and the combination was heated up until all of the ingredients had been transformed into a product, as verified by (TLC). Once the process was completely satisfied to have ended, the combination was permitted to settle at room temperature **[16]**.

L_1:color: pale green, molecular formula $C_8H_8N_4S$ (192.18) mp:175-177 ºC. Anal. Calcd (%): C, 49.92, H, 4.22, N, 29.07; found (%): C, 49.94, H, 4.16, N, 29.13. IR (KBr, ν cm^{-1}, (**Fig.S1**): 3289 (NH_2), 3146 (N─H), 2905 (Ar-H), 1617 (C=N). ^{1}HNMR δ-DMSO-d_6: 7.67 (s, 1H, NH), 7.46-7.24 (m, 5H, ArH+NH), 7.1-7.09 (s, 2H, NH_2). ^{13}C NMR δ-DMSO d_6: 170.15, 158.48, 152.38, 130.69, 125.88, 122.45, 121.22, 119.02 (**Figs.S2, and S3**).

L_2:color: pale yellow, molecular formula $C_{10}H_8N_4OS$ (232.21) mp: 210-212 ºC. Anal. Calcd (%): C, 51.77, H, 3.43, N, 24.18;found (%): C, 51.7, H, 3.44, N, 24.10. IR (KBr, ν cm^{-1}, **Fig.S4**): 3248 (N─H), 3170 (N─H), 2962 (Ar-H), 1591 (C=N). ^{1}HNMR δ-DMSO-d_6: 12.66 (s, 1H, OH), 8.41-8.34 (d, 4H, ArH), 8.01 (s, 1H, NH), 7.78 (s, 1H, NH), 7.50-7.38 (d, 1H, CH). ^{13}C NMR δ-DMSO-d_6: 165.12, 158.59, 156.72, 148.96, 135.62, 127.45, 124.32, 122.19, 120.21, 80.10. (**Figs.S5, and S6**).

L_3:color: pale yellow, molecular formula $C_{13}H_{12}N_4S$ (256.35), mp: 235-238 ºC. Anal. Calcd (%): C, 60.95, H, 4.77, N, 21.93;found (%): C, 60.9, H, 4.7, N, 21.9. IR (KBr, ν cm^{-1}, **Fig.S7**): 3181 (N─H), 2988 (Ar-H), 1600 (C=N). ^{1}HNMR δ in DMSO-d_6: 11.84 for (s, 1H, NH), 7.90 (s, 1H, ArH), 7.61 (s, 1H, ArH), 7.39 (s, 1H, ArH), 7.22 (s, 1H, ArH), 6.85 (s, 1H, CH), 1.19 (m, 6H, CH_3).^{13}C NMR δ in DMSO-d_6 166.28, 160.98, 157.42, 155.18, 149.77, 127.45, 126.34, 119.21, 117.86, 103.12, 22.10 (**Figs.S8, and S9**).

2.3. Preparation of [Fe(L)] complexes

The FeL_1, FeL_2, and FeL_3 complexes were synthesized by putting 1.5 mmoles of $Fe(NO_3)_3.9H_2O$ (0.6 g) dissolved in (20 mL) of EtOH to (3.0 mmol) of L_1 and L_2 (3.0 mmol, 0.58 g of L_1, and 0.70 g of L_2) in separate flasks respectively, and DMF solution of $Fe(NO_3)_3.9H_2O$ (1.5 mmoles, 0.6 g) was added to L_3 (3.0 mmol, 0.77 g of L_3), dissolved in (15 mL) of DMF and few drops of piperidine then stirred under reflux for 2-3 hrs to get three red, dark red and brown precipitates (Scheme 1). These precipitates were filtered out, washed with ethanol, and dried in a desiccator at decreased pressure.

[**FeL_1**] (red); $[Fe(NO_3)_2(L_1)_2].(NO_3)(2H_2O)$.: Molecular formula $C_{16}H_{20}N_{11}O_{11}S_2Fe$ (662.3), decomp.t: >300ºC. Anal. Calcd (%): C, 29.1, H, 3, N, 23.3, found (%): C, 29.09, H, 2.99, N, 23.31, Λm: 62.8 (Ω^{-1} cm^2 mol^{-1}), IR (KBr pellet, ν cm^{-1}): 3122 (N─H), 1604 (C=N), 1528 (N═O), 430 (M─N) and 560 (M─O).

[**FeL_2**] (dark red); $[Fe(NO_3)_2(L_2)_2].NO_3$: Molecular formula $C_{20}H_{16}N_{11}O_{11}S_2Fe$ (706.4), decomp.t: 271ºC. Anal. Calcd (%): C, 34.01, H, 2.3, N, 21.79, found (%): C, 34.06, H, 2.34, N, 21.77, Λm: 58.3 (Ω^{-1} cm^2 mol^{-1}), IR (KBr pellet, ν cm^{-1}): 3156 (N─H), 1533 (C=N), 1402 (N═O), 450 (M─N) and 555 (M─O).

[**FeL_3**] (brown); $[Fe(NO_3)_2(L_3)_2].(H_2O)(NO_3)$: Molecular formula $C_{26}H_{26}N_{11}O_{10}S_2Fe$ (772.5), decomp.t: >300ºC. Anal. Calcd (%): C, 40.45, H, 3.42, N, 19.87, found (%): C, 40.49, H, 3.44, N, 19.89, Λm: 57.34 (Ω^{-1} cm^2 mol^{-1}), IR (KBr pellet, ν cm^{-1}): 3170 (N─H), 1578 (C=N), 1652 (N═O), 448 (M─N) and 540 (M─O).

2.4. Kinetic investigations into prepared coordination compounds

As a way to comprehend more about the Arrhenius parameters, which include the frequency factor (A), entropy of activation (S*), enthalpy of activation (H*), and free energy of activation (G*), one efficient methodology is to investigate the kinetics and thermodynamics of the thermal deterioration procedure. When attempting to determine the kinetic parameters mentioned above using TGA curves [17-19], the Coats-Redfern approach was used:

$$Log\left[\frac{Log\left(\frac{W\infty}{W\infty-w}\right)}{T^2}\right] = Log\left[\frac{AR}{\emptyset E^*}\left(1-\frac{2RT}{\emptyset E^*}\right)\right] - \frac{E^*}{2.303RT} \quad (1)$$

Where W represents the mass loss independent of temperature T, W∞ represents the mass retention after the breakdown phase, and φ represents the heated frequency. A chart of formula (1)'s left side against 1/T would produce a straight line

since 1-2RT/E*≈1. subsequently using the intercept and slope, it became conceivable to identify the Arrhenius constant, A. The other kinetic parameters, ΔS*, ΔH*and ΔG*, were calculated using the following equations

$$\Delta S^* = 2.303R \log \frac{Ah}{K_B T}$$

$$\Delta H^* = E^* - RT$$

$$\Delta G^* = \Delta H^* - T\Delta S$$

Where, K_B and h are Boltzmann's and Planck's constants, respectively.

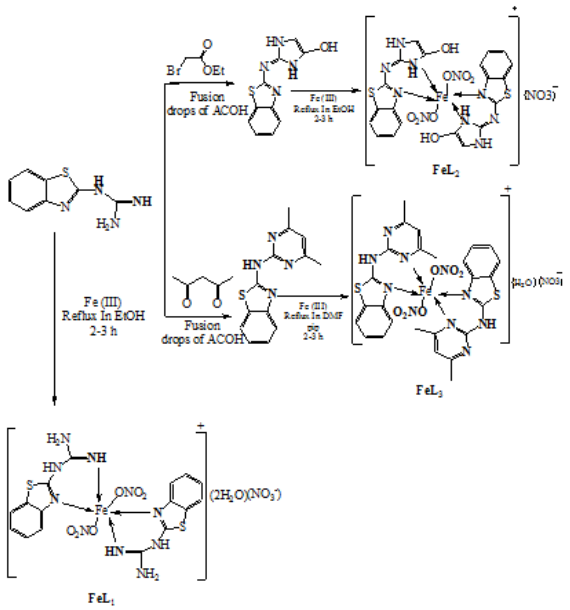

Scheme 1. Preparation of complexes FeL_1, FeL_2 and FeL_3.

2.5. Spectrophotometric studies

Regarding the intention of evaluating UV-Vis spectra between 200 and 700 nm, stock solutions of metal chelates at 1×10^{-3} Mol/L have been generated by combining a specific amount of the metal chelates in DMF.

2.6. Catalytic application

2.6.1. Procedure for synthesizing of 7-amino-4,5-dihydro-tetrazolo[1,5-a]pyrimidine-6-carbonitrile derivatives

At ambient temperature, a stirrer with magnets was applied for mixing 10 mol % of the FeL_2 complex in 20 mL of EtOH/H_2O (v/v) (1/3) solution. Aromatic aldehyde **1a-i** (1 mmol), Malononitrile **2** (1 mmol, 60 mg), and 5-aminotetrazole **2** (1 mmol, 85 mg) were then combined. A sufficient period of time was stipulated for the reaction mixture to reflux (**Scheme 3**). The mixture utilized throughout the procedure was permitted to settle to room temperature. After the conversion of reactant into product, which is determined by thin layer chromatography (TLC). Acetone was added to the reaction mixture to recover the iron complex catalyst then ethyl acetate was used to obtain the organic material, and the resulting 7-amino-4,5-dihydro-tetrazolo[1,5-*a*]pyrimidine-6-carbonitrile derivatives **4a–i** organic phases were then washed with water and dried over anhydrous Na_2SO_4 and the final crude product was obtained by rotatory evaporator. The refined compounds were obtained *via* recrystallizing the consequent solid compound with EtOH to acquire it, which was subsequently verified by its melting point, FT-IR, ^{1}H-NMR, and ^{13}C-NMR spectra (See Supporting Information **Fig.14S:22S**).

2.6.2. The spectral data of the selected compounds are as follows

Compound 4a: mp = 220–223ºC. IR (KBr, ν cm^{-1}) = 3229 (NH_2), 2210 (CN), ^{1}H-NMR (400 MHz, DMSO-d_6) δ = 10.83 (s, 1H, NH), 7.50-7.52 (d, *J* = 8.2 Hz, 2H, ArH), 7.43-7.39 (m, *J* = 8.2 Hz, 3H, ArH), 7.33 (s, 2H, NH_2), 5.15 (s, 1H, CH). ^{13}C-NMR-(DMSO-d_6) δ = 159.07, 158.24, 149.52, 135.43, 134.25, 132.84, 131.05, 117.75, 79.43. Anal. Found for $C_{11}H_9N_7$: C, 55.22; H, 3.79; N, 40.98. Calc: C, 55.20; H, 3.78; N, 40.96.

Compound 4b: mp = 230–232ºC. IR (KBr, ν cm^{-1}) = 3246 (NH_2), 2207 (CN), ^{1}H-NMR (400 MHz, DMSO-d_6) δ = 10.49 (s, 1H, NH), 7.80-7.78 (d, *J* = 8.0 Hz, 2H, ArH), 7.61-7.59 (d, *J* = 8.0 Hz, 2H, ArH), 7.42(s, 2H, NH_2), 5.46 (s, 1H, CH). ^{13}C-NMR-(DMSO-d_6) δ = 157.61, 155.34, 153.88, 145.92, 132.96, 132.54, 131.29, 118.67, 81.55. Anal. Found for $C_{11}H_8N_7Cl$: C, 48.27; H, 2.95; N, 35.83. Calc: C, 48.26; H, 2.95; N, 35.81.

Compound 4c: mp = 238–241ºC. IR (KBr, ν cm^{-1}) = 3260 (NH_2), 2204 (CN), ^{1}H-NMR (400 MHz, DMSO-d_6) δ = 10.45 (s, 1H, NH), 8.02-7.95 (d, *J* = 8.1 Hz, 2H, ArH), 7.81-7.79 (d, *J* = 8.1 Hz, 2H, ArH), 7.51 (s, 2H, NH_2), 5.31 (s, 1H, CH). ^{13}C-NMR-(DMSO-d_6) δ = 158.30, 156.88, 147.55, 135.40, 134.25, 132.68, 132.10, 119.79, 82.92. Anal. Found for $C_{11}H_8N_7Br$: C, 41.53; H, 2.53; N, 30.82. Calc: C, 41.50; H, 2.52; N, 30.80

Compound 4d: mp = 215–218ºC. IR (KBr, ν cm^{-1}) = 3238 (NH_2), 2206 (CN), ^{1}H-NMR (400 MHz, DMSO-d_6) δ = 11.15 (s, 1H, NH), 8.30-8.28 (d, *J* = 7.9 Hz, 2H, ArH), 7.99-7.97 (d, *J* = 7.9 Hz, 2H, ArH), 7.69 (s, 2H, NH_2), 5.13 (s, 1H, CH), 3.12 (s, 3H, CH_3). ^{13}C-NMR-(DMSO-d_6) δ = 155.08, 154.39, 147.72, 134.17, 133.21, 132.94, 132.07, 117.34, 72.68, 61.65. Anal. Found for $C_{12}H_{11}N_7O$: C, 53.53; H, 4.12; N, 36.41 Calc: C, 53.51; H, 4.11; N, 36.39.

Compound 4e: mp = 221–224ºC. IR (KBr, ν cm^{-1}) = 3268 (NH_2), 2211 (CN), ^{1}H-NMR (400 MHz, DMSO-d_6) δ = 11.13 (s, 1H, NH), 8.43-8.24 (d, *J* = 8.1 Hz, 2H, ArH), 8.16-8.05 (d, *J* = 8.1 Hz, 2H, ArH), 7.78 (s, 2H, NH_2), 5.73 (s, 1H, CH), 3.18 (s, 3H, CH_3). ^{13}C-NMR-(DMSO-d_6) δ = 158.42, 155.64, 151.78, 145.48, 132.63, 131.29, 130.86, 130.12, 129.93, 118.31, 77.93, 68.36. Anal. Found for $C_{12}H_{11}N_7O$: C, 53.54; H, 4.13; N, 36.43. Calc: C, 53.53; H, 4.13; N, 36.40.

Compound 4f: mp = 245–248ºC. IR (KBr, ν cm^{-1}) = 3218 (NH_2), 2209 (CN), ^{1}H-NMR (400 MHz, DMSO-d_6) δ = 10.28 (s, 1H, NH), 8.21-7.98 (d, *J* = 7.9 Hz, 2H, ArH), 7.96-7.85 (d, *J* = 7.9 Hz, 2H, ArH), 7.73 (s, 2H, NH_2), 5.62 (s, 1H, CH). ^{13}C-NMR-(DMSO-d_6) δ = 159.16, 158.42, 152.28, 143.70, 135.39, 134.45, 133.52, 119.92, 83.62. Anal. Found for $C_{11}H_8N_8O_2$: C, 46.48; H, 2.84; N, 39.42. Calc: C, 46.46; H, 2.84; N, 39.40.

Compound 4g: 238–240ºC. IR (KBr, ν cm^{-1}) = 3252 (NH_2), 2203 (CN), ^{1}H-NMR (400 MHz, DMSO-d_6) δ = 11.09 (s, 1H, NH), 7.96-7.41 (m, 4H, ArH), 7.40 (s, 2H, NH_2), 5.71 (s, 1H, CH). ^{13}C-NMR-(DMSO-d_6) δ = 159.40, 152.36, 151.67, 147.56, 141.89, 132.95, 131.20, 130.16, 118.35, 76.47. Anal. Found for $C_{11}H_8N_8O_2$: C, 46.48; H, 2.83; N, 39.42. Calc: C, 46.46; H, 2.84; N, 39.40.

Compound 4h: mp = 230–232ºC. IR (KBr, ν cm^{-1}) = 3268 (NH_2), 2205 (CN), ^{1}H-NMR (400 MHz, DMSO-d_6) δ = 10.68

(s, 1H, NH), 8.42-8.04 (m, 3H, ArH), 7.48 (s, 2H, NH_2), 5.18 (s, 1H, CH). ^{13}C-NMR-(DMSO-d_6) δ = 157.18, 135.38, 148.97, 136.53, 134.46, 132.08, 130.05, 119.24, 82.11. Anal. Found for $C_9H_7N_7O$: C, 47.16; H, 3.08; N, 42.78. Calc: C, 47.16; H, 3.06; N, 42.75.

Compound 4i: 248–250ºC. IR (KBr, ν cm^{-1}) = 3236 (NH_2), 2210 (CN), ^{1}H-NMR (400 MHz, DMSO-d_6) δ = 10.41 (s, 1H, NH), 7.54-7.05 (m, 3H, ArH), 6.51 (s, 2H, OCH_2), 5.24 (s, 1H, CH), 3.69 (s, 2H, NH_2). ^{13}C-NMR-(DMSO-d_6) δ = 159.57, 155.46, 148.78, 144.08, 136.26, 134.32, 132.55, 117.92, 80.03, 73.22. Anal. Found for $C_{12}H_9N_7O_2$: C, 50.88; H, 3.20; N, 34.62. Calc: C, 50.86; H, 3.18; N, 34.60.

2.6.3. Recovery and reusing of catalysts

A homogeneous catalyst (FeL_2) is easily reusable more than once after being segregated by precipitation in acetone following each catalytic operation is complete. Before being dried for 3 hours at 90ºC, the removed catalyst needs to be cleaned with EtOH and bi-distilled H_2O. A catalyst may often be used again in another process attributable to its recyclability.

3. Results and Discussion

3.1. General properties

The results of the analysis revealed the chemical formulae for the complexes of FeL_1, FeL_2, and FeL_3. The best matching was 2L:1M for all colored compounds. The range of conductivity readings was 57.2–62.4 (Ω^{-1} cm^2 mol^{-1}), which is consistent with mono-electrolyte complexes [28].

3.2. IR, ^{1}H NMR Spectrum

The functional groups of the ligand are recognized using the FT-IR spectroscopic technique, which also offers proof of interactions between those groups and the central metal ions of the novel complexes **[20]. Figures (1S, 4S, and 7S)** display the distinctive FT-IR spectral bands for the L_1, L_2, and L_3 ligands and their corresponding FeL_1, FeL_2, and FeL_3 chelates **Figures (10S, 11S, and 12S)**.

The L_1 ligand's spectra exhibited a band at 3145 cm^{-1}, which is associated with the ν(NH) vibration; nevertheless, interaction with Fe-metal ions caused this peak to recede to an interval of 3122–3125 cm^{-1} in the complexes **[21]**. The C=N group initially appeared at 1617 cm^{-1} in the free ligand but was altered to 1604 cm^{-1} after coordination with Fe^{3+}. Furthermore, the FeL_1 complex exhibits two further bands at 560 and 430 cm^{-1} in evidence of M-O and M-N bonding. The ν(NH) group and the ν(C=N) group, accordingly, have connections with the bands at 3249 cm^{-1} and 1592 cm^{-1}, respectively, in the FT-IR spectra of the L_2. The resultant peak transformed to lower frequencies in the FT-IR spectra of the FeL_2 complex, where ν(NH) arose at 3156 cm^{-1} and ν(C=N) emerged at 1533 cm^{-1}. The formation of the FeL_2 metal complex was demonstrated by the appearance of M-O and M-N bands at 557 cm^{-1} and 448 cm^{-1}, respectively **[22].** The center ring nitrogen atom coordinated to the metal ion in the FeL_3 complex, where two absorption bands vibrating at 3182 and 1600 cm^{-1} were ascribed to ν(NH) and ν(C=N), and the peak exhibited a shift to 11-17 cm^{-1} **[23].** Metal-O and M-N bonds in the FeL_3 complex are attributed to absorptions measured at 537 and 435 cm^{-1}, respectively. These outcomes show that the preparation of FeL complexes was effective. The NO^{3-} ions are coordinated to the metal ion as unidentate for all the prepared complexes. Each unidentate nitrate group possesses three non-degenerated modes of vibrations, which appeared at 1418–1398, 1316–1317, and 810-813 cm^{-1}, respectively. The νs(NO^{3-}) of the unidentate NO^{3-} is markedly shifted to lower frequencies compared to that of the free nitrate (1700–1800 cm^{-1}) **[24].** To ascertain the structure of the ligand and its complex, ^{1}H NMR spectra of the ligands are recorded in DMSO-d_6 (**Fig. 2S, 5S, and 8S**).

In the (L_1) ligand's ^{1}H-NMR spectra, there was 1 signal for (NH) at 7.67 and 5 signals for (5H, ArH+NH) at 7.46-7.24 and 7.09 for (NH_2) respectively. The singlet at 12.3 ppm in (L_2) ^{1}H NMR is caused by the ligand's OH proton, while NH was present at 8.01 and 7.78 ppm and CH at 7.39. Additional identifying clues came from the protons of the aromatic rings of the benzothiazole and imidazole molecules, which were present in ratios between 8.41 and 8.34 ppm. ^{1}H NMR spectra of complex FeL_3 showed (NH) at 11.84, 7.90-7.22 (4H, ArH), 6.85 (CH), and 1.19 (m, 6H, $2CH_3$).

3.3. Electronic spectra for FeL complexes

The L_1, L_2, and L_3 ligands' UV-visible spectra in DMF fluids display three bands with wavelengths between 228 and 330 nm that may be attributed to the π→π*, n→π*, and intra ligand bands, respectively (Fig. 1) **[25].** Each of the ligand's electronic transitions inside the metal orbitals and the inclusion of Fe metal ions induce significant changes, which point to the creation of the complex **[26].** According to charge transfer between the ligand and the metal, new bands were found in the range of 329–399 nm in Fe complexes **[27]**. Furthermore, the d → d transition in the FeL_1, FeL_2, and FeL_3 complexes was recorded at 422, 420, and 419 nm which was assigned to Octahedral geometry **[27].**

Molar conductance information for prepared Fe metal chelates are 62.8, 58.3, and 57.3 Ω^{-1} mol^{-1}cm^2 showing that mono electrolyte nature was detected for the produced FeL_1, FeL_2, and FeL_3 respectively **[28].**

3.4. Mass Spectrometry

The metal chelate's molecular ion excesses were employed as evidence for the suggested formulations. (**Fig.13S**). The FeL_1 mass spectrum gave the peak of the molecular ions assigned to [M$^+$] at m/z 662 amu (13%) and confirmed the proposed formula $[C_{16}H_{20}N_{11}O_{11}S_2)Fe]$. FeL_1's suggested fragmentation peaks are provided as an illustration in (**Scheme 2**). The base peak that emerges at m/z = 68 is $[C_5H_8]$. There were peaks at 614.27 (24.4%), 564.88 (14.31%), 192 (24.08%), 177 (55.12%), 150 (30.12%), and 93 (35.12%) that were prompted by different segments. The mass spectrum of FeL_2 revealed the molecular ion peak associated with [M+] at m/z = 706 amu (17%), supporting the suggested formula $[C_{20}H_{16}N_{11}O_{11}S_2)Fe]$. The hypothesized formula $[C_{26}H_{26}N_{11}O_{10}S_2)Fe]$ was supported by the molecular ion peak at m/z = 772.5 amu (15.5%) in the mass spectrum of FeL_3.

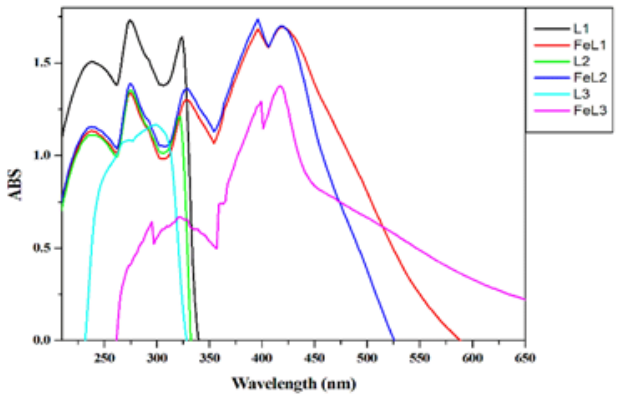

Fig.1 UV–vis scanning of Fe metal chelates in DMF media at 25 °C.

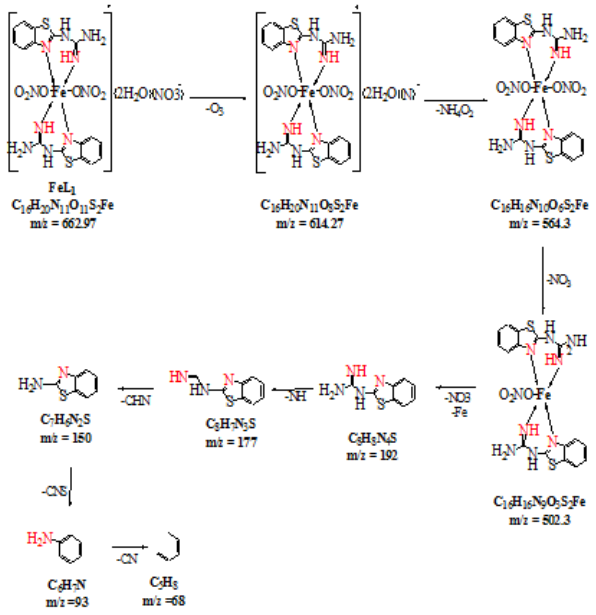

Scheme 2. Fragmentation pathway of FeL_1, below each structure, the precise masses of the particles and their chemical formulas are displayed.

3.5. Magnetic moment

The magnetic susceptibility of FeL_1, FeL_2, and FeL_3 was deduced from the orbital or spinning motion of the central metal ion, Fe^{3+} ion. The deduced values were found to be m_{eff} = 5.49, 5.47, and 5.53 B.M for FeL_1, FeL_2 and FeL_3, respectively. These findings led to consideration of these compounds' paramagnetic behavior and the proposal of their octahedral geometry **[29].** The para-magnetic features could interpret the magnetic character of the current Fe-complexes due to the electronic configuration of d_5 orbitals of Fe^{3+} ion and support their octahedral geometrical structures.

3.6. Thermal Analysis

Thermal analysis, which provides crucial details on compounds' thermal properties, phases of thermal deterioration, types of intermediary molecules, and remaining products of thermal degradation, represents one of the foremost beneficial instruments used to forecast the molecular structure and stability of substances **[30].** Anionic groups connected to the metal center, as well as the amount and kind of water and/or organic solvent molecules, must be understood. Complexes' TGA temperature charts and the thermogram assessment conclusions are shown in (**Table 1S**). It is evident from the TGA thermograms that the under-investigation compounds broke down in sequential five stages (as with the FeL_1 complex) and four steps (as with the FeL_2 and FeL_3 complexes). The FeL_1 complex first broke down in five separate processes across the temperatures of 46-171, 172-282, 283-354, 355-521, and 522-711 ºC. The water molecule ($2H_2O$) was lost in the first stage, resulting in a decrease in weight of 14.7% of the overall mass (calculated value is 14.8%). The piece of $N_7O_6H_7$ was lost in the second period with a decrease in mass of 30.35% (calculated value is 30.36%). The weight loss of the CH divide in the third stage, which accounted for 1.9% of the total weight loss, was evaluated. The fourth step is with a missing $C_8N_3S_2$ piece. The last performance had a mass loss of C_5H_8 and left a 12.2% Fe and 2C residue at 715 ºC. The FeL_2 compound underwent four sequential rounds of thermal breakdown. The first step involved the loss of NO_3 molecules embedded in the structures of the complexes and went from ambient temperature to 156ºC. The second stage, which began at 160ºC and proceeded up to 207ºC, saw the disintegration of organic molecules as well as the loss of coordinated NO_3 molecules. The $C_6H_4N_5O_5$ fragment lost as much as 32% of the complex weight in the third phase. The following phases in the breakdown process resulted in the loss of the $C_9H_5N_2S_2$ portions of the ligand, leaving a residue of the metal+CH after the decomposition reaction at 600ºC. Since certain metal complexes may require a higher temperature to completely decompose their organic ligand, the leftovers at 600ºC retained some of the organic ligands. FeL_3 was revealed to detect the following four steps The 2.3% transpiration of moisture in the Fe-complex was presumably accountable for the loss within the range of 55-215°C **[31, 32].** The second reduction in weight was detected progressively between 215 and 357 ºC, which was thought to be caused by the nitrate and a portion of the organic moiety in FeL_3 degrading by 65%. With $C_4H_6N_2$ degradation and a loss percentage of 10.6%, the third stage's weight loss was seen in the range of 357–560ºC. As indicated in (Table 1S), the fourth degradation stage (564–742ºC) involved the elimination of some ligands by an 8% (calcd=8.01%) mass loss, leaving a residue of 13.5% that was analyzed to contain the fragment 4C and metal.

3.7. Formation constant, stability constant, and Gibbs free energy of the prepared complexes

The formation constants (K_f) and stability constant pK (**Table 1**) were estimated and the values were arranged in this manner: **FeL_2 > FeL_1 > FeL_3**. Furthermore, Gibbs free energy (ΔG*) contemplated for complexes proven negative adequate to exemplify evolution's spontaneity of complexation reaction.

3.8. FeL complex's catalytic performance

3.8.1. Synthesis of 7-amino-4,5-dihydro-tetrazolo[1,5-*a*]pyrimidine-6-carbonitrile 4a-i derivatives.

Iron complexes have been shown to exhibit promising catalytic activity in a wide range of chemical reactions. This is

mainly due to the unique properties of transition metals, including their ability to undergo various processes and coordinate with multiple ligands. Furthermore, the catalytic activity of iron complexes can be impacted by variations in ligand structures and substituents. Recent studies have focused on exploring the effects of different ligand structures and substituents on the catalytic properties of iron complexes. As a demonstration, a new catalytic multi-component reaction involving aromatic aldehyde **1a** (1 mmol), 5-aminotetrazole **2** (1 mmol), and malononitrile **3** (1 mmol), was chosen for synthesizing 7-amino-4,5-dihydro-tetrazolo[1,5-*a*]pyrimidine-6-carbonitrile derivative **4a**. The condensation mechanism was explored beneath the influence of significant factors involving catalyst amount on yield, solvent utilized, time, and distinctive Lewis acid and basic catalysts on catalytic activity to establish the best reaction conditions. Without a catalyst, the process of condensation requires an extended amount of time to complete. The addition of FeL_2 improves product yield and speeds up reaction time, as indicated in (**Scheme 3**). Electrophilic substitution processes can successfully and efficiently synthesize several aromatic aldehydes, as indicated in (**Scheme 3**).

Table 1: The values of the synthesized metal complexes formation constant (K_f), stability constant (pK), and Gibbs free energy Δ(G*) at 298 K.

Complex	Type of complex	K_f	pK	ΔG^* ($KJmol^{-1}$)
FeL_1	1:2	7.48×10^7	7.87	-44.20
FeL_2	1:2	9.55×10^7	7.98	-45.52
FeL_3	1:2	6.25×10^7	7.79	-44.47

3.8.2. Catalyst loading effects

The specific type of solvent used during the synthesis procedures has had a significant impact on the catalytic potential of the FeL_2 complex **[34–35].** To synthesize 7-amino-4,5-dihydro-tetrazolo[1,5-*a*]pyrimidine-6- carbonitrile derivatives catalyzed by Fe(L_2), the effects of several solvents, including acetone, trichloromethane, CH_3CN, and DMF (N, N-dimethylformamide), were examined and summarized in (**Table 3**). The results demonstrate that solvent type has a major impact on synthesis by demonstrating that polar protic solvents (MeOH, EtOH, AcOH, H_2O, and EtOH/H_2O) greatly outperform aprotic solvents ($CHCl_3$, DMF, CH_3CN, THF, and DCM). While ethanol/H_2O (1:3) provided the maximum amount of product (**Table 3**) (97 catalyzed by FeL_2, respectively), EtOH and H_2O are efficient solvents (93% and 90% catalyzed by FeL2. In other solvents (DMF and THF), the product yields were low for both synthesis and catalysts. This mixture was preferred because it is green, safe, cheap, and gives us the highest yield in comparison with organic solvents.

3.8.3. Effect of solvents

The influence of the catalyst quantity on the product yield is shown in (**Table 2**). It has been noted that increasing the catalyst ratio of FeL_2 lengthens the catalytic synthesis process and increases the yield of the 7-amino-4,5-dihydro-tetrazolo[1,5-*a*]pyrimidine-6-carbonitrile derivative. The product yield jumped from 16% to 97% by increasing the catalyst dose from 3 to 10 mol%. The coordinated ligands to the Fe (III) ion's electronic and steric properties have a significant impact on the catalytic potential of the Fe complex catalyst **[33]**. As seen in earlier work by our research group, the coordinated ligand L_2 appears to have an unanticipated impact on the steric and electronic catalytic potential of FeL_2 **[12-15]**.

Table 2: Amount of catalyst used for the synthesis of 7-amino-4,5-dihydro-tetrazolo[1,5-*a*]pyrimidine-6-carbonitrilederivative **4a.**

Entry	Cat. mol (%)	Yield (%)
1	4	16
2	5	28
3	6	55
4	7	72
5	8	81
6	9	93
7	10	97
8	11	97

[a] Reaction conditions: **1a** (1 mmol), **2** (1 mmol), **3** (1 mmol), and Catalyst (10 mol%) FeL_2 in a mixture of water and ethanol (3:1 ratio) were refluxed 15 min.
[b] Isolated yields based on **4a**.

Table3: Effect of solvent on synthesis of 7-amino-4,5-dihydro-tetrazolo[1,5-*a*]pyrimidine-6-carbonitrile derivatives **4a**

Solvent	Time(min)	Yield (%)
THF	60	49
$CHCl_3$	60	55
CH_3CN	60	58
DMF	60	59
ACOH	30	79
H_2O	15	90
EtOH	15	93
H_2O/EtOH	15	97

[a] Reaction conditions 1a (1 mmol), 2 (1 mmol), 3 (1 mmol), and catalyst (10 mol%) in a mixture of ethanol and water (1:3 ratio) were refluxed 15 min.
b Isolated yields based on 4a..

3.8.4 | Catalyst effects caused by various Lewis acid, basic, or ionic liquids

FeL_2 complex has also been investigated as a mild Lewis acid catalyst for various chemical transformations and has received a lot of attention recently. In the absence of a catalyst and under the same conditions, a trace product was produced by the reaction of benzaldehyde, 5-amino tetrazole, and malononitrile (**Table 4, 1**). In the chosen reaction conditions, various Lewis acids including $Mg(OTf)_2$, $MnCl_2.4H_2O$,$AlCl_3$, $MgCl_2$, MnO_2, $Zn(OTf)_2$, $CuCl_2$, $TiCl_4$, and $FeCl_3.6H_2O$ are tested. It was proven that the FeL_2 catalyst outperformed all other Lewis acids that were water-stable by a wide margin (**Table 4, 2–12**). FeL_2 was found to be the most effective catalyst and afforded the desired product **4a** in 97% yield (**Table 4, 13-15**).

3.8.5. Recycling of catalyst

The capacity of the catalytic systems to segregate and recover from the reaction mixture constitutes one of their greatest benefits. Along with contributing to being industrialized, this benefit also complies with the fundamentals of green chemistry. Therefore, numerous studies were performed to determine if the generated hybrid FeL_2 homogeneous catalyst could be reused and recycled to create variants of the 7-amino-4,5-dihydrotetrazolo[1,5-*a*]pyrimidine-6-carbonitrile. The FeL_2-catalyst was ditched from the resulting mixture by precipitation in acetone, washed with water and ethanol, dried, and reclaimed in additional reactions after the full transformation of starting material into a product (monitored through thin-layer chromatography [TLC] had occurred. The yield of isolated products has not significantly decreased after five successive runs, as shown in (**Fig. 2**), and the FeL_2-catalyst has maintained its effectiveness and stability during these experiments. The FT-IR spectra of the FeL_2-catalyst before and after being used in the process five times demonstrate that no specific structural changes have been produced, indicating that it may be used as a stable and recyclable catalyst in organic reactions (**Fig. 3**).

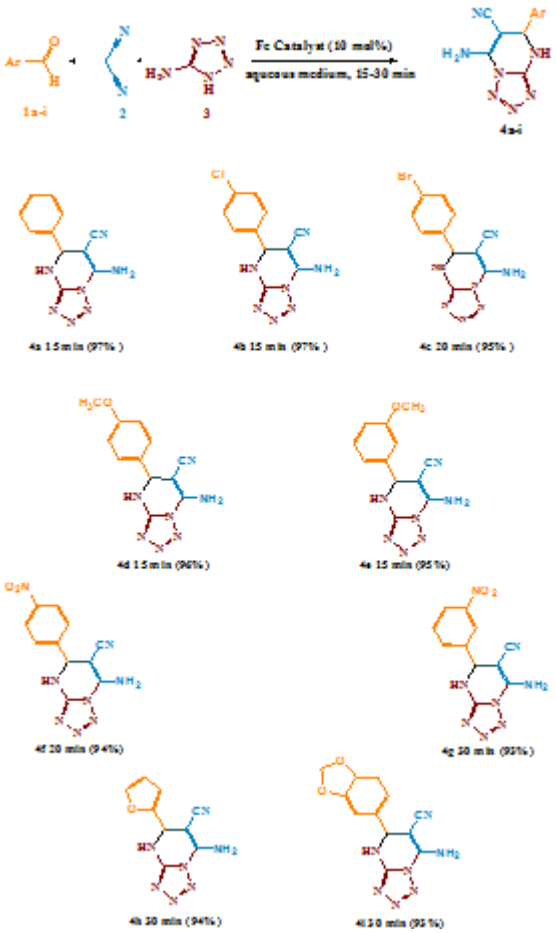

Scheme 3: 7-amino-4,5-dihydro-tetrazolo[1,5-*a*]pyrimidine 6-carbonitrile derivatives **4a–i**- time of reaction (min) and yield (%).

3.8.6. Predicted mechanism for Catalytic behavior in the synthesis procedure

Using a one-pot, three-component interaction with aromatic aldehydes, 5-aminotetrazole, and malononitrile, (**Scheme 4**) showed the proposed process for the synthesis of 7-amino-4,5-dihydro-tetrazolo[1,5-*a*]pyrimidine-6-carbonitrile derivatives. The hypothesized process contains four main phases that are based on the literature: tautomerization, intramolecular cyclization, Michael addition, and Knoevenagel condensation. Aldehyde and (NH_2) of aminotetraole combine to form the molecule (A) by a catalyzed Knoevenagel condensation. As can be observed, a double bond is formed when the hybrid FeL_2 catalyst activates the CHO groups in the aldehyde (1) and (NH_2) of the amino tetrazole. Malononitrile (3) then attacks this intermediate (A), creating intermediate (B), by attacking the double bond with CH_2. Furthermore, the intramolecular Michael addition between the NH and CN groups of the intermediate molecule B resulted in the formation of an intermediate product C, which was further converted to a final product 4a-i through isomerization [36].

Table 4: Use of different Lewis acids for the reaction **4a**.

Entry	Cat. (mol%)	Conditions[a]	Yield (%)
1	no. catalyst	H_2O/EtOH, 1 day	Trace
2	$FeCl_2.6H_2O$ (5)	H_2O/EtOH , 15 min	44
3	$FeCl_3.6H_2O$ (10)	H_2O/EtOH , 15 min	54
4	$Fe(OTf)_3$ (10)	H_2O/EtOH , 15 min	65
5	$MgCl_2$ (10)	H_2O/EtOH , 15 min	54
6	$Mg(OTf)_2$ (10)	H_2O/EtOH , 15 min	47
7	$MnCl_2.4H_2O$ (10)	H_2O/EtOH , 15 min	61
8	MnO_2 (10)	H_2O/EtOH , 15 min	59
9	$Zn(OTf)_2$ (10)	H_2O/EtOH , 15 min	46
10	$CuCl_2$(10)	H_2O/EtOH , 15 min	53
11	$TiCl_4$ (10)	H_2O/EtOH, 15 min	48
12	p-TsOH (10)	H_2O/EtOH , 15 min	55
13	FeL_1 (10)	H_2O/EtOH , 15 min	96%
14	FeL_3 (10)	H_2O/EtOH , 15 min	95%
15	FeL_2 (10)	H_2O/EtOH , 15 min	97%

[a] Reaction conditions **1a** (1 mmol), **2** (1 mmol), **3** (1 mmol), and catalyst (0.1 mmol) in amixture of water and ethanol (3:1) were refluxed 15 min.
[b] Isolated yields based on **4a**.

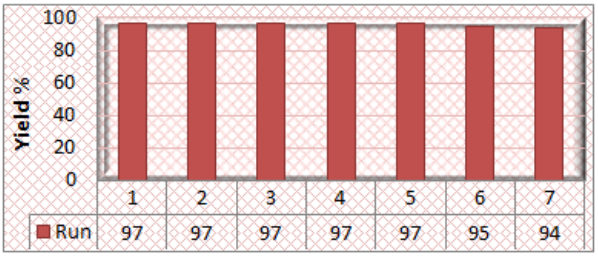

Fig. 2: Recyclability of FeL_2 in the model reaction

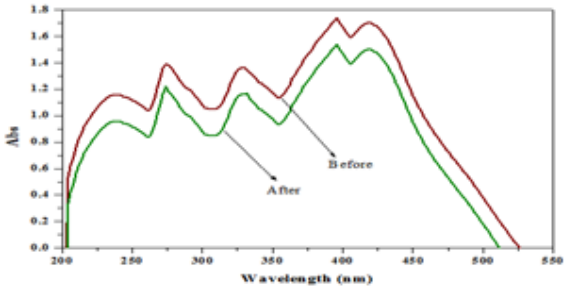

Fig. 3: Molecular electronic spectra of FeL_2 catalyst before and after the investigated catalytic reaction.

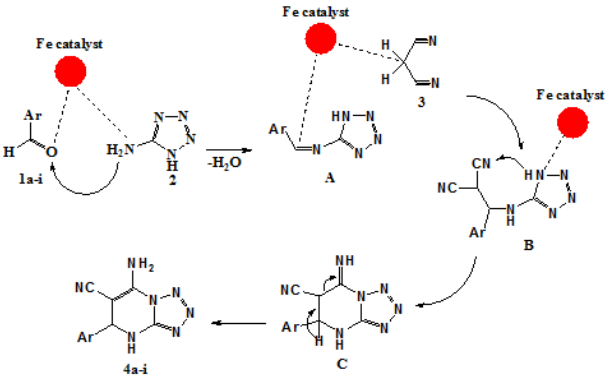

Scheme 4. Recommended process for production of 7-amino-4,5-dihydro-tetrazolo[1,5-*a*] pyrimidine-6-carbonitrile derivatives

4. Conclusion

The new approach to thesynthesis of 7-amino-4,5-dihydro-tetrazolo[1,5-*a*]pyrimidine-6-carbonitrile derivatives was carried out using a one-pot, three-component reaction between 5-aminotetrazole, various substituted aromatic aldehydes, and malononitrile under mild reaction conditions by using FeL_2 complex as a green and sufficient catalyst. Conventional techniques including FT-IR, ^{1}H-NMR, ^{13}C-NMR, mass spectra, electronic spectra, and TGA were utilized to characterize the produced FeL complexes. Results demonstrate significant stability and structures aligned with desired outcomes. In conclusion, theFeL_2 complex was designed and developed using a straightforward procedure. A comprehensive method of the reaction pathway reveals that the FeL_2 complex plays a crucial role in enabling the desired outcome with excellent product yields (95–97%). Tested under various conditions, this catalyst emerged as the most effective for this specific reaction. The FeL complex was compared with other Lewis acids and bases the results show that the FeL_2 complex is more efficient and offers higher yield and purity. The mild reaction conditions, quick reaction times (15–30 min), straightforward procedure, ease of isolation from the reaction mixture, and reused at least five times without significantly losing its catalytic activity are just a few of the appealing benefits of this protocol.

CRediT authorship contribution statement:

Mahmoud Abd El Aleem Ali Ali El-Remaily: Conceptualization, Methodology, Project administration, Supervision. *Omar Elhady*: Investigation, Supervision. *Thomas Nady A.Eskander*: Methodology, Writing – original draft. *Shaaban K. Mohamed*: Methodology. *Ahmed Abu-Dief*: Methodology, Supervision.

Data availability statement

The data that support the findings of this study are available in the supporting file and the corresponding author upon reasonable request.

Declaration of competing interest

The authors declare that they do not have any competing financial interests or personal relationships that could have appeared to influence the findings reported in this paper.

References

[1] A. Dömling, I. Ugi, *Angew. Chem. Int. Ed.* 39 (2000) 3168-3210.
[2] V. Nair, A.U. Vinod, C. Rajesh, *J. Org. Chem.*, 66 (2001) 4427–4429.
[3] B. List, C. Castello, *Synlett*., 11 (2001) 1687–1689.
[4] R. Medimagh, S. Marque, D. Prim, J. Marrot, Chatti S. Concise, *Org. Lett*., 11 (2009) 1817–1820.
[5] B. H. Babu, K. Vijay, K. B. M. Krishna, N. Sharmila, M. B. Ramana, *J. Chem. Sci*. 128 (2016) 1475–1478.
[6] M. Vafaeezadeh, M. Hashemi, *M. J. Mol. Liq*., 207 (2015) 73–79.
[7] M.A.A. El-Remaily, H.A. Hamad, A.M.M. Soliman, O. Elhady, *Appl Organomet Chem.*, 35 (2021) e6238.
[8] M.A.A. El-Remaily, A.M.M. Soliman, M.E. Khalifa, N.M. El-Metwaly, A. Alsoliemy, T. El-Dabea, A.M. Abu-Dief, *Appl Organomet. Chem.*, 36 (2022) e6320.
[9] M. Zare, L. Moradi, *Appl. Organomet. Chem.*, 35 (2021) e6358.
[10] G.S. Rani, M. Vijay, L.A.B.P. Devi, *Chemistry Select*, 4 (2019) 10133– 10142.
[11] M.A.A. El-Remaily, T. El-Dabea, M. Alsawat, H.H.M. Mohamed, A.A. Alfi, N. El-Metwaly, A.M. Abu-Dief, *ACS Omega* 6 (2021) 21071−21086.
[12] M.A.A. El-Remaily, O.M. Elhady, *Tetrahedron Lett*., 57 (2016) 435.
[13] E.K. Shokr, M.S. Kamel, H. Abdel-Ghany, M.A.A. El-Remaily, *Curr. Res. Green Sustain. Chem.*, 4 (2021), 100090.
[14] E.A. Ahmed, A.M.M. Soliman, A.M. Ali, M.A.A. El-Remaily, *Appl. Organometal. Chem*. (2021) 35.
[15] M.A.E.A.A. El-Remaily, *Chin. J. Cata* 36 (2015) 1124.

[16] A.M. Soliman, K.Sh. Mohamed, M.A.E.A.A.A. El-Remaily, and H. Abdel-Ghanya, *J. Heterocyclic Chem*., 51 (2014) 1202.
[17] L.H. Abdel Rahman, A.M. Abu-Dief, N.A. Hashem, A.A. Seleem, *Int. J. Nanomater. Chem.*, 1 (2015) 79.
[18] L.H. Abdel-Rahman, A.M. Abu-Dief, S.K. Hamdan, A.A. Seleem, *Int. J.Nanomater*. Chem., 1(2015) 65.
[19] A.W. Coats, I.P. Redfern, *Nature*, 20 (1964) 68.
[20] K.M. Ibrahim, R.R. Zaky, E.A. Gomaa, L.A. Yasin, *J. Mol. Struct.*, 1101 (2015) 124.
[21] A. Uçar, M. Findik, N. Koçak, A.T. Çolak, O.S. ahin, *Cumhuriyet Sci. J.*, 42 (2021) 22.
[22] M. Tyagi, S. Chandra, P. Tyagi, *Spectrochim. Acta A.*, 117 **(**2014**)** 1.
[23] Y.Q. Lu, Z.H. Deng, *Practical Infrared Spectrum Parse, Publishing House of Electronics Industry*, Beijing, 1989.
[24] A.A.A. Emara, *Spectrochim. Acta A*., 77 **(**2010**)** 117.
[25] A.M. Abu-Dief, R.M. El-khatib, F.S. Aljohani, S.O. Alzahrani, A. Mahran, M.E. Khalifa, N.M. El-Metwaly,J. Mol. Struct. 1242 (2021) 130693.
[26] A.D. Khalaji, S.M. Rad, G. Grivani, D. Das, *J.Calorim.*, 103 (2011) 747–751.
[27] S.D. Al-Qahtani, A. Alsoliemy, S.J. Almehmadi, K. Alkhamis, A.F. Alrefaei, R. Zaky, N. El-Metwaly, *J. Mol. Struct.*, 1244 (2021) 131238.
[28] W.H. Mahmoud, N.F. Mahmoud , Gehad G. Mohamed, *Appl. Organometal. Chem*. 31 (2017) e3858.
[29] S.A. Aly, *J. Radiat. Res. Appl. Sci.*, 3 (2017) 163.
[30] W.J. Geary, *Coord. Chem. Rev*., 7(1971) 81.
[31] H. Sharma, H. Mahajan, B. Jamwal, S. Paul, *Catal Commun.*, 107 (2018) 68–73.
[31] S. Anuma, P. Mishra, B.R. Bhat, *J. Taiwan Inst. Chem. Eng*., 95 (2019) 643–51.
[33] M.A.A. El-Remaily, O.M. Elhady, *Appl. Organometal. Chem*., 33 (2019) e4989.
[34] G. Grivani, V. Tahmasebi, A.D. Khalaji, K. Fejfarova, M. Dusˇek, *Polyhedron*, 51 (2013) 54–60.
[35] M.M. Heravi, H.M. Tehrani, K. Bakhtiari, A.H. Oskooie, *Catalysis Communications*, 8 (2007) 1341–1344.
[36] K. Ablajan, W. Kamil, A. Tuoheti and S. Wan-Fu, *Molecules*, 17 (2012) 1860-1869.